引用格式：WEN Han, XU Peng, PI Liangwen, et al. Generation of Femtosecond Magnetic Pulses by Circularly Polarized Vortex Laser-driven Plasma[J]. Acta Photonica Sinica, 2023, 52(9):0932001
温寒,徐鹏,皮良文,等.圆偏振涡旋激光脉冲驱动等离子体产生飞秒磁脉冲的研究[J].光子学报,2023,52(9):0932001

# 圆偏振涡旋激光脉冲驱动等离子体产生飞秒磁脉冲的研究

温寒[1,2],徐鹏[1],皮良文[1],付玉喜[1]
(1 中国科学院西安光学精密机械研究所 阿秒科学与技术研究中心,西安 710119)
(2 中国科学院大学 光电学院,北京 101408)

**摘 要**:飞秒磁场脉冲对研究超快磁化、超快退磁、超快磁存储和自旋超快动力学等过程具有重要意义。传统的脉冲磁场受限于脉冲电源性能无法获得毫秒量级以下的超短脉冲磁场,无法研究飞秒尺度的磁动力学过程。利用超短脉冲激光驱动等离子体产生旋转电流是目前产生飞秒磁场脉冲的有效方法。本文利用质点网格法模拟圆偏振拉盖尔高斯光束驱动等离子体中的电子运动从而产生光电流以及飞秒磁脉冲的过程,模拟产生了特斯拉量级的飞秒超短磁脉冲,并系统讨论了驱动激光强度与等离子体密度对磁脉冲的影响。结果表明,脉冲磁场的脉宽与驱动光一致,其强度随着激光场强度、等离子体密度增加而增加。通过本文研究寻找产生飞秒磁脉冲的优化实验参数,有望将超快磁动力学研究推进到飞秒时间尺度。

**关键词**:飞秒磁场脉冲;拉盖尔高斯光束;圆偏振涡旋激光;激光-等离子体相互作用;Particle-In-Cell方法
**中图分类号**:O437 **文献标识码**:A **doi**:10.3788/gzxb20235209.0932001

## 0 引言

脉冲磁场的研究最早可以追溯至20世纪初,传统的方案是使用脉冲电源提供瞬时电流进而产生脉冲磁场,通过优化磁体结构以及磁体与电源的配置,可以实现高达100 T的磁场强度[1]。但是产生强脉冲磁场的传统方法对脉冲电源的性能和磁体的机械强度要求高,相应的实验设施尺寸大、造价高,并且产生的磁场脉冲宽度最短只能达到5 ms左右,很难产生更短的磁场脉冲。随着激光技术的发展,利用激光和等离子体相互作用为产生强磁场提供了新的方案,通过使用具有轨道角动量的强激光束与等离子体相互作用,可以将轨道角动量从激光转移到电子上形成螺线电流,进而产生超强的轴向磁场[2]。例如,时银从理论上研究了利用不同频率和轨道角动量的涡旋光来驱动电子产生螺线电流,从而可以产生40 T的磁场[3]。NUTER R等使用$2\times10^{18}$ W/cm$^2$相对论强度的涡旋光与等离子体作用,通过理论计算预测可以产生100 T的脉冲磁场[4]。上述研究中传统方案产生的强磁场脉冲的脉冲宽度为毫秒量级,具有轨道角动量的强激光和等离子体相互作用产生的强磁场为准静态磁场,两种方案都无法研究超快磁动力学过程[5]。

为了获得更短的强磁场脉冲,FREEMAN M R等使用飞秒激光触发光导奥斯顿开关的方案,在共面波导中产生了瞬态电流,进而获得了皮秒时间尺度的磁场脉冲[6]。然而,由于脉冲的衰减时间由材料的载流子寿命决定,未掺杂GaAs的典型寿命为100到500 ps,而低温生长的GaAs的寿命可能只有几皮秒[7],因此采用上述方法最多只能产生皮秒量级的磁场脉冲。HILLEBRANDS B等将皮秒磁场脉冲作用于共线铁磁样品中,通过Dzyaloshinskii-Moriya作用来产生单个斯格明子,同时,该工作还利用皮秒磁场脉冲实现了相反

**基金项目**:国家自然科学基金(No. 92050107)
**第一作者**:温寒,wenhan20@mails.ucas.edu.cn
**通讯作者**:皮良文,lwpi@opt.ac.cn;付玉喜,fuyuxi@opt.ac.cn
**收稿日期**:2023-04-10;**录用日期**:2023-05-23

极性斯格明子的受控切换[8-9]。近年来，在铁磁薄膜的有关的实验中观察到章动运动。进动运动下，铁磁材料的磁化开关时间大约为20 ps，由于章动频率远高于进动频率，因此章动运动有利于更快的磁化开关，大约为亚皮秒量级[10]。

飞秒磁脉冲可以研究更快的自旋动力学过程，例如铁磁材料Co的瞬态磁化过程受自旋输运效应的控制，自旋极化的激发电子的寿命为飞秒量级，激发电子在外场中自旋进动也处在飞秒时间尺度[11-12]。利用光学二次谐波探测到Au表面激发的载流子自旋极化过程是百飞秒量级，而且发现Fe表面激发的载流子寿命也为百飞秒量级[13]。NiO和Ru的退磁时间和电子-声子弛豫时间在百飞秒量级[14-16]。目前实验上还无法产生飞秒磁脉冲，极大限制了超快磁动力学和自旋动力学的深入研究。

本文利用质点网格法(Particle-In-Cell, PIC)和Smilei程序模拟了真空环境下圆偏振拉盖尔高斯(Laguerre-Gaussian，LG)光束与均匀分布的等离子体靶相互作用的过程[17-18]。电流密度分布表明，粒子在激光场中的径向运动中获得角动量，可以产生0.5至50 T峰值强度，脉冲宽度为10 fs左右的磁场。PIC模拟结果表明，可以通过控制激光束强度和等离子体密度来增加脉冲磁场强度。

## 1 激光与等离子体靶相互作用模型

利用Smilei程序进行三维PIC模拟，模拟环境为真空环境，模拟窗口$x\times y\times z$为160 $\lambda_0\times$40 $\lambda_0\times$40 $\lambda_0$，模拟网格d$x$、d$y$、d$z$为0.1 $\lambda_0$，其中$\lambda_0$为激光波长，每个网格内有4个宏粒子。每个宏粒子可以看成多个等离子体粒子的集合体，宏粒子密度的物理意义是单位网格体积内一个宏粒子所代表的粒子密度。等离子体密度单位为$N_r\equiv\varepsilon_0\cdot{\omega_0}^2\cdot m_e/e^2$，其中$\varepsilon_0$为介电常数，$\omega_0$为激光角频率，$m_e$为电子质量，$e$为电子电荷量。电流密度是由宏粒子数密度、电荷数和电子速度相乘而得到，其单位为$J_r\equiv ceN_r$，其中$c$为电磁波在真空中的传播速度。

在模拟过程中，边长为30 $\lambda_0$的正方体等离子体靶位于模拟窗口内部左侧，圆偏振LG光的焦平面与模拟窗口左端平齐。一般情况下，激光从无穷远处传来，然后进入模拟窗口。但在模拟过程中，为了节省计算时间，同时为保证初始时刻的激光脉冲不会进入模拟窗口而对等离子体靶产生扰动，将圆偏振LG光的脉冲中心设置于模拟窗口左侧18 $\lambda_0$处。激光入射等离子体靶的方式为垂直入射，激光沿着$x$方向传播，传播轴在$yz$平面的位置是$y$=20 $\lambda_0$，$z$=20 $\lambda_0$，采用的激光光束为圆偏振LG光束[19-22]，激光方程为

$$E=a_0\frac{W_0}{W(x)}\left[\frac{\rho}{W(x)}\right]^{|l|}L_m^{|l|}\left[\frac{2\rho^2}{W(x)^2}\right]\exp\left[-\frac{\rho^2}{W(x)^2}\right]\cdot\exp\left[\mathrm{j}\omega_0 t-\mathrm{j}kx-\mathrm{j}l\varphi-\mathrm{j}k\frac{\rho^2}{2R(x)}+\right.$$
$$\left.\mathrm{j}(l+2m+1)\arctan\left(\frac{2x}{k{\omega_0}^2}\right)\right]\cdot\left(i\hat{e}_y+s\hat{e}_z\right)\cdot F(t-x/c) \tag{1}$$

BAUMANN C研究了不同拓扑数组合的激光对驱动产生的电子束的影响[19]。模拟结果显示，当激光模式参数[$l$,$m$,$s$]组合设置为[0,−2,−1]时，可获得理想螺旋电子束。因此，本文也将激光拓扑数[$l$,$m$,$s$]组合设置为[0,−2,−1]。式(1)中$a_0\equiv eE_0/m_e\omega_0 c$表示无量纲电场强度，其中$E_0$为激光所对应的电场强度，$L_m^{|l|}$表示拉盖尔多项式，$s$表示激光的偏振度($s$=−1表示右旋圆偏光)，束腰$W_0$为10 $\lambda_0$，$k$为激光的波数，激光波长$\lambda_0$为800 nm。高斯时间包络函数为$F(t-x/c)\equiv\exp\left[-4\ln 2\left(t-x/c\right)^2/\tau^2\right]$，其中激光脉冲电场的半高全宽$\tau$为3倍的激光周期$t_0$[23]。

对于波长为800 nm的驱动激光，等离子体临界密度为$N_{\mathrm{cr}}\equiv\varepsilon_0\cdot{\omega_0}^2\cdot m_e/e^2\equiv 1.74\times10^{21}\ \mathrm{cm}^{-3}$，本文模拟的等离子体密度为1.74×10$^{18}$至8.7×10$^{20}$ cm$^{-3}$，低于临界密度以保证激光能够顺利穿透等离子体靶。在模拟过程中仅考虑电子密度引起的折射率变化，不考虑非线性效应，并假设离子不移动，且等离子体的初始速度和初始温度均为0，这样可以减少离子的集体效应对电子动力学的影响。

## 2 仿真模拟结果与分析

### 2.1 激光脉冲与等离子体相互作用产生磁脉冲

等离子体密度$n_0$设置为1.74×10$^{18}$ cm$^{-3}$，光强$I_0$设置为1.93×10$^{21}$ W/cm$^2$时，脉冲宽度$\tau$为3倍的激光周

期 $t_0$。图 1(a)～(d)是当 $t$ 分别处于不同时刻，模拟窗口内宏粒子的密度分布图。对比发现，激光与等离子体相互作用后，粒子束呈螺旋状分布并沿 $x$ 轴运动。从图中可以看出，电子运动过程中，极少数电子运动至模拟窗口边界外，但大量的电子分布在长时间的作用下是稳定的，因此可以忽略模拟窗口外的电子运动。对于模拟窗口内的电子分布，可以用有质动力模型来描述这种径向约束[24-25]。LG 光束与经典的高斯光束不同，LG 光束的中心处光强最低，因此存在一个势阱。有质动力势与光场强度梯度成正比，有质动力势阻止位于势阱中的电子径向逃逸，从而可以产生具有飞秒持续时间的结构电子束。激光脉冲进入模拟窗口 430 fs($t$=160 $t_0$)后，电流密度的 PIC 模拟结果如图 1(e)所示，电流密度 $J_\theta$ 分布呈环形，说明在激光-等离子体相互作用过程中，电子的角向运动产生环形电流。

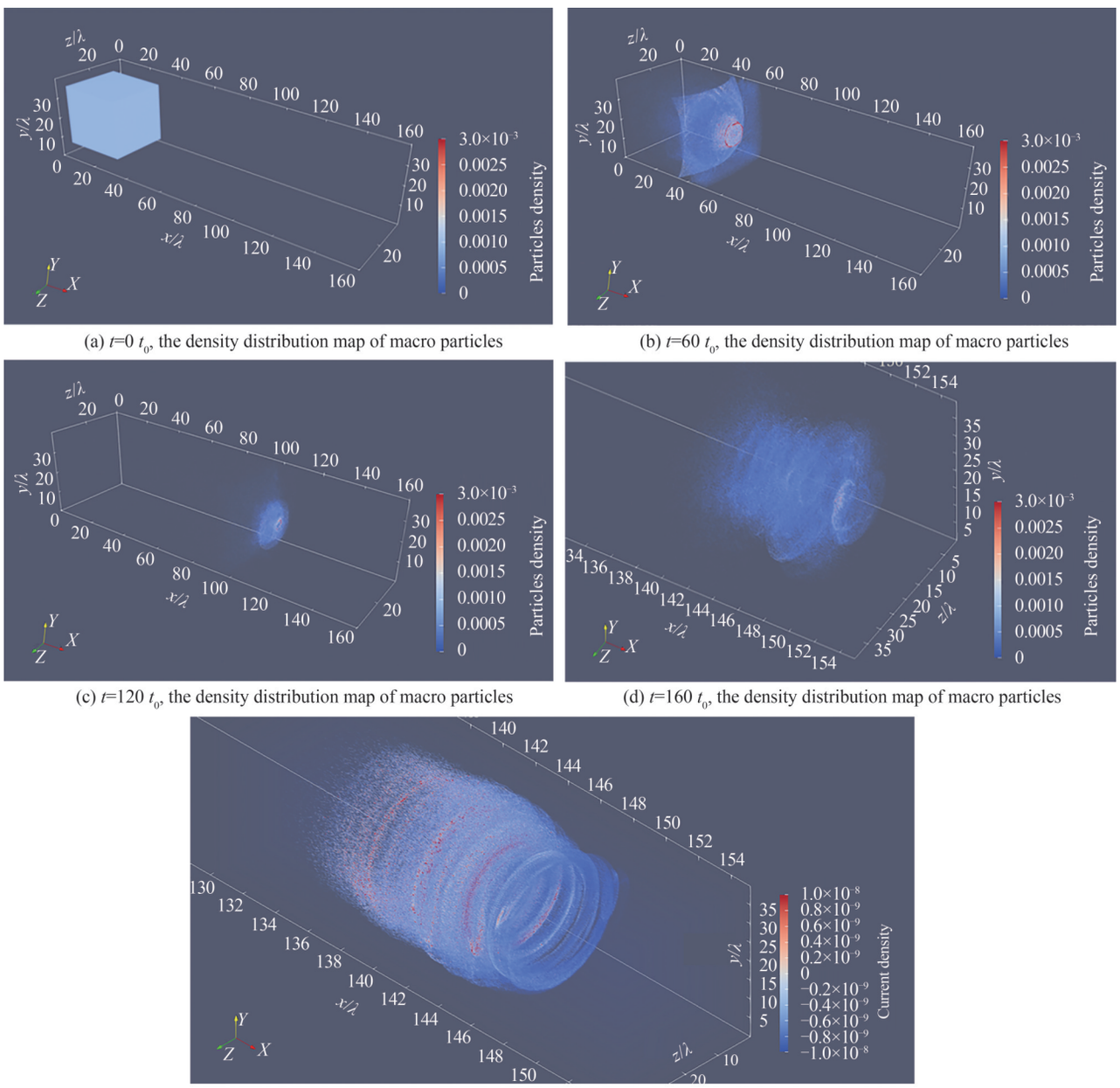


(a) $t$=0 $t_0$, the density distribution map of macro particles

(b) $t$=60 $t_0$, the density distribution map of macro particles

(c) $t$=120 $t_0$, the density distribution map of macro particles

(d) $t$=160 $t_0$, the density distribution map of macro particles

(e) $t$=160 $t_0$, $J_\theta$ current density distribution diagram

图 1　宏粒子的密度分布与电流密度分布

Fig.1　Density distribution of macro-particles and current density distribution

根据电流的磁效应，环形电流可以产生磁场。激光脉冲进入模拟窗口 430 fs 后，图 2 为感生磁场 $B_x$ 的 PIC 模拟结果。由图 2 可知，利用超短脉冲激光产生了 6 T 的轴向磁脉冲，且 $B_x$ 的脉冲宽度约为 10 fs，与激光脉冲的脉冲宽度保持一致。

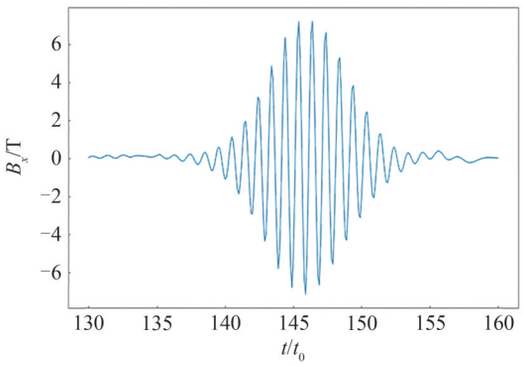


图 2 在 $x=145\,\lambda_0$，$y=25\,\lambda_0$ 时，感生磁场 $B_x$ 随时间 $t$ 的变化

Fig.2 $x=145\,\lambda_0$, $y=25\,\lambda_0$, diagram of induced magnetic field $B_x$ as a function of $t$

### 2.2 激光强度和等离子体密度对磁脉冲强度的影响

产生磁脉冲的过程主要是由于激光-等离子体相互作用引起的，超短脉冲激光与等离子体相互作用能够激发等离子体中电子的集体运动，从而使等离子体中的带电粒子获得能量。激光强度与等离子体密度是激光与物质相互作用中的两个重要参数，我们分别选择不同的激光强度和等离子体密度，研究两个参数对感生磁脉冲强度的影响。

#### 2.2.1 激光强度对磁脉冲强度的影响

等离子体密度 $n_0$ 设置为 $1.74\times10^{18}\ \mathrm{cm^{-3}}$，在不改变激光其他参数的情况下，改变光强 $I_0$ 从 $8.57\times10^{16}$ 增加至 $1.93\times10^{21}\ \mathrm{W/cm^2}$ 时，研究磁场 $B_x$ 随着输入光强 $I_0$ 和输入磁场强度 $B_0$ 变化。由图 3(a)可知，$B_x$ 正比于 $B_0$，通过 $I_0\equiv\sqrt{\varepsilon_0/\mu_0}\,E_0^{\,2}/2$ 和 $B_0=E_0/c$，可知 $B_0$ 正比于 $\sqrt{I_0}$，得出 $B_x$ 正比于 $\sqrt{I_0}$ 的结论，与图图 3(b)相符。感生磁场强度 $B_x$ 正比于电流密度分布 $J_\theta$。再由电流密度定义可知，电流密度正比于电子运动速度。同时，洛伦兹力驱使电子运动，电子运动的速度正比于洛伦兹力，而洛伦兹力正比于输入磁场强度 $B_0$，因此 $B_x$ 正比于 $B_0$。

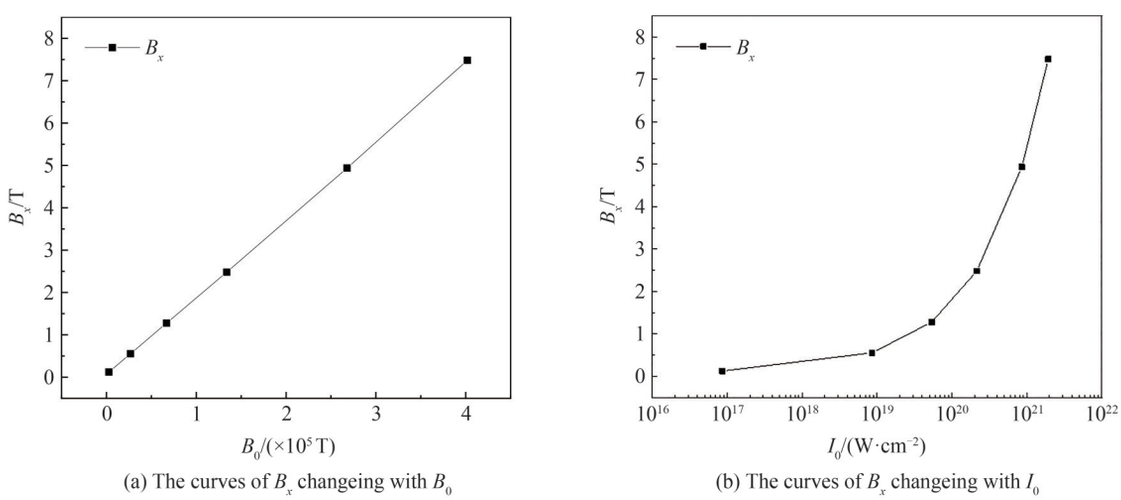


(a) The curves of $B_x$ changeing with $B_0$

(b) The curves of $B_x$ changeing with $I_0$

图 3 感生磁场 $B_x$ 随输入磁场强度 $B_0$ 和输入光强 $I_0$ 变化

Fig.3 The curves of the induced magnetic field $B_x$ changing with the input magnetic field strength $B_0$ and input laser intensity $I_0$

#### 2.2.2 等离子体密度对磁脉冲强度的影响

将光场强度设置为 $1.93\times10^{21}\ \mathrm{W/cm^2}$，在不改变激光参数的情况下，改变等离子体密度，将 $n_0$ 从 $1.74\times10^{18}$ 增加至 $8.7\times10^{20}\ \mathrm{cm^{-3}}$。如图 4 所示，$B_x$ 随 $n_0$ 的增加而增加。这是由于随着等离子体靶密度的增加，电流密度随之增加，因此产生的磁脉冲强度也增加。从图 4 中可以看出，可以产生 0.5 至 50 T 峰值强度的轴向磁脉冲，并且发现当等离子体密度小于 $10^{20}\ \mathrm{cm^{-3}}$ 时，$B_x$ 的强度变化不大，但随着等离子体密度大于 $10^{20}\ \mathrm{cm^{-3}}$ 时，$B_x$ 增幅较大。由于电流密度与等离子体密度也成正比，因此磁场 $B_x$ 随等离子体密度增加而增加。

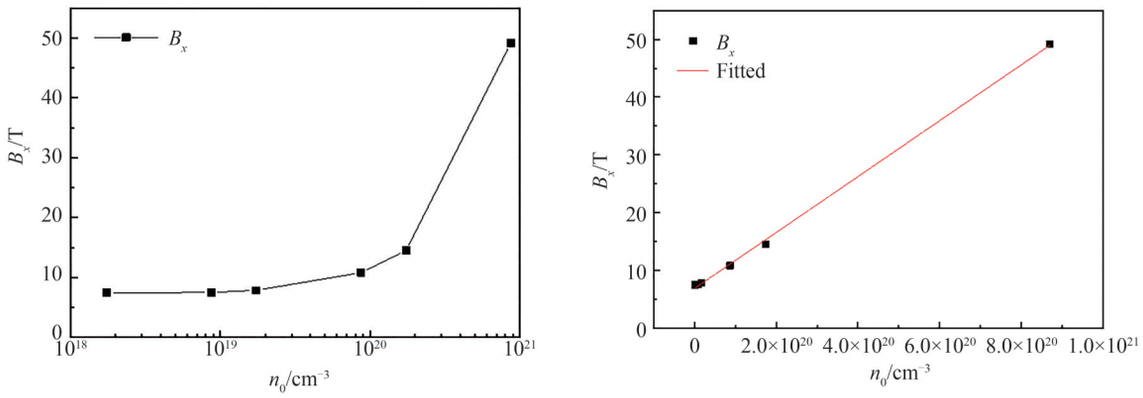


(a) The curves of $B_x$ changeing with $n_0$　　(b) $B_x$ linearly fitted with the change of $n_0$

图4　感生磁场$B_x$随着等离子体密度$n_0$变化曲线和线性拟合

Fig.4　The induced magnetic field $B_x$ changes with the plasma density $n_0$, and the curve is fitted linearly

## 3　结论

本文利用PIC模拟方法和Smilei程序对相对论光强的超短脉冲激光与等离子体相互作用产生涡旋电子束进而产生脉冲磁场这一物理过程进行了系统的模拟，并产生了0.5至50 T峰值强度和10 fs左右的超短磁脉冲。通过等离子体宏粒子数密度分布、电流密度分布以及磁场强度分布探究了磁脉冲的产生过程。模拟结果表明，脉冲磁场强度与激光强度的平方根和等离子体密度成正比，通过增加电子密度和激光光强获得超短强磁场，为实验产生飞秒磁脉冲提供数值参考。以上的模拟结果有望推进超强超短磁脉冲进入飞秒超快时间尺度，为超快磁动力学和超快自旋动力学研究中控制磁性材料中电子运动、自旋等微观过程、超快自旋电子磁存储应用和磁化开关发展方面提供支撑。

**参考文献**

[1] PENG Tao, LI Liang. The status and future development of pulsed high magnetic fields[J]. Physics, 2016, 45(1): 11-18.
彭涛, 李亮. 脉冲强磁场技术发展现状与趋势[J]. 物理, 2016, 45(1):11-18.

[2] HU L X, YU T P, LU Y, et al. Dynamics of the interaction of relativistic Laguerre-Gaussian laser pulses with a wire target[J]. Plasma Physics and Controlled Fusion, 2019, 61(2): 025009-025027.

[3] SHI Y, VIEIRA J, TRINES R M G M, et al. Magnetic field generation in plasma waves driven by copropagating intense twisted lasers[J]. Physical Review Letters, 2018, 121(14):145002-145009.

[4] NUTER R, KORNEEV P, THIELE I, et al. Plasma solenoid driven by a laser beam carrying an orbital angular momentum[J]. Physical Review E, 2018, 98(3):033211-033220.

[5] CHEN Y, XU C, XU B, et al. Chirality-activated mechanoluminescence from aggregation-induced emission enantiomers with high contrast mechanochromism and force-induced delayed fluorescence[J]. Materials Chemistry Frontiers, 2019, 3(9):1800-1806.

[6] FREEMAN M R, BRADY M J, SMYTH J. Extremely high frequency pulse magnetic resonance by picosecond magneto-optic sampling[J]. Applied Physics Letters, 1992, 60(20):2555-2557.

[7] KEIL U D, DYKAAR D R. Ultrafast pulse generation in photoconductive switches[J]. IEEE Journal of Quantum Electronics, 1996, 32(9):1664-1671.

[8] FLOVIK V, QAIUMZADEH A, NANDY A K, et al. Generation of single skyrmions by picosecond magnetic field pulses[J]. Physical Review B, 2017, 96(14):140411-140421.

[9] HEO C, KISELEV N S, NANDY A K, et al. Switching of chiral magnetic skyrmions by picosecond magnetic field pulses via transient topological states[J]. Scientific Reports, 2016, 6(1):27146-27157.

[10] WINTER L, GROßENBACH S, NOWAK U, et al. Nutational switching in ferromagnets and antiferromagnets[J]. Physical Review B, 2022, 106(21):214403-214415.

[11] AESCHLIMANN M, BAUER M, PAWLIK S, et al. Ultrafast spin-dependent electron dynamics in fcc Co[J]. Physical Review Letters, 1997, 79(25):5158-5161.

[12] WIECZOREK J, ESCHENLOHR A, WEIDTMANN B, et al. Separation of ultrafast spin currents and spin-flip scattering in Co/Cu(001) driven by femtosecond laser excitation employing the complex magneto-optical Kerr effect[J]. Physical Review B, 2015, 92(17):174410-174418.

[13] MELNIKOV A, RAZDOLSKI I, WEHLING T O, et al. Ultrafast transport of laser-excited spin-polarized carriers in Au/Fe/MgO (001)[J]. Physical Review Letters, 2011, 107(7):076601-076606.
[14] ZHURAVLEV M Y, TSYMBAL E Y, JASWAL S S. Exchange model for oscillatory interlayer coupling and induced unidirectional anisotropy in $[Pt/Co]_3$/NiO$[Pt/Co]_3$ multilayers[J]. Physical Review Letters, 2004, 92(21):219703-219705.
[15] LIU Z Y, ADENWALLA S. Oscillatory interlayer exchange coupling and its temperature dependence in $[Pt/Co]_3$/NiO/$[Co/Pt]_3$ multilayers with perpendicular anisotropy[J]. Physical Review Letters, 2003, 91(3):037207-037215.
[16] HELLWIG O, BERGER A, FULLERTON E E. Domain walls in antiferromagnetically coupled multilayer films[J]. Physical Review Letters, 2003, 91(19):197203-197207.
[17] DEROUILLAT J, BECK A, PÉREZ F, et al. Smilei: a collaborative, open-source, multi-purpose particle-in-cell code for plasma simulation[J]. Computer Physics Communications, 2018, 222(17):351-405.
[18] ARBER T D, BENNETT K, BRADY C S, et al. Contemporary particle-in-cell approach to laser-plasma modelling[J]. Plasma Physics and Controlled Fusion, 2015, 57(11):113001-113028.
[19] BAUMANN C, PUKHOV A. Electron dynamics in twisted light modes of relativistic intensity[J]. Physics of Plasmas, 2018, 25(8):083114-083122.
[20] WENG Xiaoyu, GUO Hanming, DONG Xiangmei, et al. Focusing characteristics of Laguerre-Gaussian radially polarized beam through high numerical aperture[J]. Acta Photonica Sinica, 2011, 40(5): 798-802.
翁晓羽, 郭汉明, 董祥美, 等. 拉盖尔高斯径向偏振光高数值孔径聚焦特性[J]. 光子学报, 2011, 40(5):798-802.
[21] ZHOU Yepeng, REN Hongliang, WANG Juan, et al. Comparative analysis of the trapping force using Laguerre Gaussian beam and Gaussian beam[J]. Acta Photonica Sinica, 2013, 42(11): 1300-1304.
周业鹏, 任洪亮, 王娟, 等. 拉盖尔高斯光束与高斯光束捕获力比较[J]. 光子学报, 2013, 42(11):1300-1304.
[22] ZHANG Hongxian, ZHAO Heng. Orbital angular momentum of high-order elliptical Hermite-Gaussian beams[J]. Acta Photonica Sinica, 2008, 37(8) :125-128.
张洪宪,赵珩. 高阶椭圆厄密-高斯光束的轨道角动量研究[J]. 光子学报, 2008, 37(8):125-128.
[23] PI L W, HU S X, STARACE A F. Favorable target positions for intense laser acceleration of electrons in hydrogen-like, highly-charged ions[J]. Physics of Plasmas, 2015, 22(9):093111-093123.
[24] GUAN Mengxue, CHEN Daqiang, HU Shiqi, et al. Theoretical insights into ultrafast dynamics in quantum materials[J]. Ultrafast Science, 2021, (4): 9767251.
[25] KONG Q, MIYAZAKI S, KAWATA S, et al. Electron bunch trapping and compression by an intense focused pulse laser[J]. Physical Review E, 2004, 69(5):056502-056513.

# Generation of Femtosecond Magnetic Pulses by Circularly Polarized Vortex Laser-driven Plasma

WEN Han[1,2], XU Peng[1], PI Liangwen[1], FU Yuxi[1]
(1 *State Key Laboratory of Transient Optics and Photonic Technology, Xi'an Institute of Optics and Fine Mechanics, Chinese Academy of Sciences, Xi'an* 710119, *China*)
(2 *School of Optoelectronics, University of Chinese Academy of Sciences, Beijing* 101408, *China*)

**Abstract**: Research on pulsed magnetic fields dates back to the early 20th century. Nowadays, ultra-short pulsed magnetic fields are being utilized to better understand ultrafast physical microprocesses, such as domain motion and spin-orbit interaction, with time scales ranging from microseconds to femtoseconds. In particular, femtosecond magnetic field pulses are of great significance for studying ultrafast magnetization, ultrafast demagnetization, ultrafast magnetic storage, and spin ultrafast dynamics. However, traditional pulsed magnetic fields are limited by the performance of the pulse power supply and the mechanical strength of the coil and cannot achieve higher pulsed magnetic field strengths. Additionally, the pulse length of the magnetic pulse generated by the pulse power supply is at the millisecond level, which makes it unsuitable for studying faster magnetic dynamics processes. Fortunately, recent studies have shown that when ultra-short pulse lasers interact with plasmas, hot electrons are produced on the surface of the plasma target. These hot electrons are then excited and pass through the target material, producing strong charge separation on the back surface of the target material. Under the action of the laser, these excited electrons are accelerated, generating strong electromagnetic radiation. Consequently, using ultra-short pulse lasers

to drive electron flows is currently the most promising method for generating femtosecond magnetic field pulses. Thus, the goal of this paper is to use a three-dimensional model to simulate the interaction between the driving optical field and the plasma target. This simulation will help to study the physical processes involved, such as the propagation of the optical field, the movement of free electrons, vortex currents, and pulse magnetic field generation. By optimizing the relevant parameters, this research aims to generate femtosecond magnetic field pulses.

In this paper, we employ the Particle-In-Cell (PIC) method as our simulation approach. This method utilizes the Vlasov-Maxwell equation set to accurately describe the self-consistent dynamics in plasma simulation. The electrons in the plasma are subject to the Lorenz force, which generates new current density as they move. This equation effectively corrects the electric and magnetic fields through the charge density and current density. The driving light described is a circularly polarized vortex beam, with a wavelength of 800 nm and an optical field intensity of approximately $10^{16}$ to $10^{21}$ W/cm$^2$. The pulse width of the beam is roughly 10 fs. The plasma density ranges from $10^{18}$ to $10^{20}$ cm$^{-3}$, and is confined within a cubic space with a side length of 30 $\lambda_0$. During the simulation process, we only consider refractive index changes due to electron density and do not account for non-linear effects. Additionally, we assume that the ions are stationary and that the initial velocity and temperature of the plasma are both 0.

During theoretical simulation, a proportionality gradient between momentum potential and the strength of the light field is created due to the lowest intensity of the vortex beam at its center. This gradient then forms a potential well, preventing electrons from escaping outward and producing a structured electron beam with a femtosecond duration. In addition, particles acquire angular momentum in their radial motion within the laser field, generating a vortex current. This in turn produces a pulsed magnetic field based on the current magnetic effect.

The simulation results indicate that when circularly polarized vortex beams, with light field intensities of the order of $10^{16}$ to $10^{21}$ W/cm$^2$, interact with plasma densities ranging from $10^{18}$ to $10^{20}$ cm$^{-3}$, they can generate ultra-short magnetic pulses with peak intensities of 0.5～50 tesla and pulse time widths of about 10 fs. The effects of driving laser intensity and plasma density on these magnetic pulses are discussed through a simulated system calculation. The results show that the pulsed magnetic field intensity is proportional to the square root of both laser intensity and plasma density. Increasing electron density and laser intensity may facilitate the generation of ultra-short strong magnetic fields, providing numerical references for the production of femtosecond magnetic pulses in experiments.

We expect that the simulation results above will facilitate the introduction of ultra-strong, ultra-short magnetic pulses into the femtosecond ultrafast realm, thereby supporting the advancement of research on ultrafast magnetic and spin dynamics, electronic motion and spin microprocessing control, ultrafast spin-electron magnetic storage applications, and magnetic switching.

**Key words**: Femtosecond magnetic field pulses; Laguerre Gaussian beam; Circularly polarized vortex laser; Laser-plasma interactions; Particle-In-Cell method

**OCIS Codes**: 320.2250; 140.7090; 260.2110; 350.5400

**Foundation item**: National Natural Science Foundation of China (No. 92050107)